epl A Letters Journal Exploring the Frontiers of Physics

November 2008

EPL, **84** (2008) 36003
doi: 10.1209/0295-5075/84/36003

www.epljournal.org

Droplet evaporation in one-component fluids: Dynamic van der Waals theory

R. Teshigawara and A. Onuki[(a)]

Department of Physics, Kyoto University - Kyoto 606-8502, Japan

received 15 June 2008; accepted in final form 18 September 2008
published online 17 October 2008

PACS 68.03.Fg – Evaporation and condensation of liquids
PACS 44.35.+c – Heat flow in multiphase systems
PACS 61.46.-w – Structure of nanoscale materials

Abstract – In a one-component fluid, we investigate evaporation of a small axysymmetric liquid droplet in the partial wetting condition on a heated wall at $T \sim 0.9T_c$. In the dynamic van der Waals theory (*Phys. Rev. E*, **75** (2007) 036304), we take into account the latent-heat transport from liquid to gas upon evaporation. Along the gas-liquid interface, the temperature is nearly equal to the equilibrium coexisting temperature away from the substrate, but it rises sharply to the wall temperature close to the substrate. On an isothermal substrate, evaporation takes place mostly on a narrow interface region near the contact line in a late stage, which is a characteristic feature in one-component fluids.

Introduction. – The wetting dynamics has been mostly studied for involatile liquids and is not well understood for volatile liquids [1]. A well-known example is evaporation of a liquid droplet on a heated substrate. Here first-order phase transition from liquid to gas occurs on the interface, where latent heat is carried away from the interface with gas flow. For a liquid droplet in air the radius $r_c(t)$ has been observed to decrease as $r_c(t) \sim (t_0 - t)^a$, with $a \cong 0.5$, until it vanishes at time t_0 [2–5]. Detailed information of evaporation and contact-line motion has been provided by various theoretical approaches [6–12]. In near-critical one-component fluids, in particular, a bubble in liquid was observed to be attracted to a heated wall even when the wall was wetted by liquid in equilibrium [13]. In one-component fluids, the contact angle increases with the heat flux.

In this letter, we numerically study evaporation of a droplet in one-component fluids in the axisymmetric geometry. As an efficient numerical method, we use the dynamic van der Waals model [14], which is a phase field model of fluids with inhomogeneous temperature. The pressure p outside a droplet (or bubble) is nearly homogeneous so that the interface temperature should be close to the equilibrium coexisting (saturation) temperature $T_{\rm cx}(p)$ even in heat flux [14,15]. Thus, near the contact line on a heated or cooled wall, a steep temperature variation and a large heat flux should appear, as theoretically studied by Nikolayev *et al.* [11,12] and as measured by Höhmann and Stephan [16]. Therefore, the hydrodynamics is singular around the contact line in heat flux. This aspect has not yet been well studied in the literature. On the other hand, in multi-component fluids, the interface temperature changes on the scale of the droplet size and evaporation should take place all over the surface.

Dynamic van der Waals model. – We examine the gas-liquid phase transition in nonstationary, inhomogeneous temperature $T(\boldsymbol{r}, t)$. We start with the entropy functional $\mathcal{S}_b$ dependent on the number density $n(\boldsymbol{r}, t)$ and the internal energy density $e(\boldsymbol{r}, t)$ and introduce $T(\boldsymbol{r}, t)$ by the functional derivative $1/T = (\delta \mathcal{S}_b/\delta n)_e$. We assume that $\mathcal{S}_b = \int \mathrm{d}\boldsymbol{r}\hat{S}$ is the space integral of the entropy density $\hat{S}$ consisting of regular and gradient parts as

$$\hat{S} = ns(n, e) - \frac{1}{2}C|\nabla n|^2, \tag{1}$$

where s is the entropy per particle dependent on n and e. The second term is the gradient entropy density, which is negative and is important near the interface. The coefficient C is assumed to be a constant. In the van der Waals theory, fluids are characterized by the molecular volume v_0 and the attractive pair interaction energy ϵ and

[(a)] E-mail: onuki@scphys.kyoto-u.ac.jp

the entropy s is written as

$$s = k_B \ln[(e/n + \epsilon v_0 n)^{3/2}(1/v_0 n - 1)] + s_0, \quad (2)$$

where $s_0/k_B = \ln[v_0(m/3\pi\hbar^2)^{3/2}] + 5/2$ with m being the molecular mass. In this letter, we assume that the fluid internal energy $\mathcal{E}_b$ is the space integral of e. Then we have the usual relation $1/T = n(\partial s/\partial e)_n$, which yields the well-known expression $e = 3nk_BT/2 - \epsilon v_0 n^2$. More generally, we may assume the form $\mathcal{E}_b = \int \mathrm{d}\boldsymbol{r}[e + K|\nabla n|^2/2]$, where the second term represents the gradient energy density [14]. In this letter, we set $K = 0$ for simplicity.

We set up the hydrodynamic equations from the principle of positive entropy production in nonequilibrium. No gravity is assumed. The mass density $\rho = mn$ obeys the continuity equation

$$\frac{\partial}{\partial t}\rho = -\nabla \cdot (\rho \boldsymbol{v}). \quad (3)$$

The momentum density $\rho\boldsymbol{v}$ and the total energy density $e_{\rm T} \equiv e + \rho\boldsymbol{v}^2/2$ are governed by [17]

$$\frac{\partial}{\partial t}\rho\boldsymbol{v} = -\nabla \cdot (\rho\boldsymbol{v}\boldsymbol{v} + \overleftrightarrow{\Pi} - \overleftrightarrow{\sigma}), \quad (4)$$

$$\frac{\partial}{\partial t}e_{\rm T} = -\nabla \cdot \left[e_{\rm T}\boldsymbol{v} + (\overleftrightarrow{\Pi} - \overleftrightarrow{\sigma}) \cdot \boldsymbol{v} - \lambda\nabla T\right]. \quad (5)$$

Here $\overleftrightarrow{\Pi} = \{\Pi_{ij}\}$ is the reversible stress tensor consisting of the van der Waals pressure $p = k_BTn/(1 - v_0 n) - \epsilon v_0 n^2$ and the gradient contribution as

$$\Pi_{ij} = p\delta_{ij} - CT\left[(n\nabla^2 n + \frac{1}{2}|\nabla n|^2)\delta_{ij} - \nabla_i n \nabla_j n\right]. \quad (6)$$

The $\overleftrightarrow{\sigma} = \{\sigma_{ij}\} = \eta(\nabla_i v_j + \nabla_j v_i) + (\zeta - 2\eta/3)\nabla \cdot \boldsymbol{v}\delta_{ij}$ is the viscous stress tensor in terms of the shear viscosity η and the bulk viscosity ζ. Hereafter $\nabla_i = \partial/\partial x_i$ with x_i representing x, y, and z. λ in eq. (5) is the thermal conductivity.

We note that Π_{ij} satisfies $\sum_j \nabla_j(\Pi_{ij}/T) = n\nabla_i\hat{\mu} - e\nabla_i T^{-1}$, where $\hat{\mu}$ is the generalized chemical potential including the gradient contribution. If C is assumed to be a constant, $\hat{\mu}$ reads

$$\hat{\mu} = T(\delta\mathcal{S}_b/\delta n)_e = \mu - TC\nabla^2 n, \quad (7)$$

where $\mathcal{S}_b = \int \mathrm{d}\boldsymbol{r}\hat{S}$ is the entropy functional and $\mu = \mu(T, n)$ is the usual chemical potential. In equilibrium the stress balance $\sum_j \nabla_j \Pi_{ij} = 0$ is equivalent to the homogeneity of $\hat{\mu}$. The interface profile $n = n(x)$ is obtained from $\mu(T, n) - CT\mathrm{d}^2 n/\mathrm{d}x^2 = \mu_{\rm cx}(T)$, where $\mu_{\rm cx}(T)$ is the chemical potential in two-phase coexistence. This interface equation was derived by van der Waals [18].

In our simulation, however, we solved the equation for the entropy density $\hat{S}$ in eq. (1),

$$\frac{\partial\hat{S}}{\partial t} + \nabla \cdot \left[\hat{S}\boldsymbol{v} - Cn(\nabla \cdot \boldsymbol{v})\nabla n - \frac{\lambda}{T}\nabla T\right] = \frac{\dot{\epsilon}_v + \dot{\epsilon}_\theta}{T}, \quad (8)$$

together with the continuity and momentum equations (3) and (4). The right-hand side of eq. (8) is the nonnegative-definite entropy production rate with

$$\dot{\epsilon}_v = \sum_{ij} \sigma_{ij}\nabla_j v_i, \quad \dot{\epsilon}_\theta = \lambda(\nabla T)^2/T. \quad (9)$$

In the literature on simulations of two-phase fluids [19–21], it is well known that a small velocity field remains nonvanishing around the interface of a droplet after long times even without heat input from the boundaries. It is an artificial *parasitic* flow and its magnitude depends on the discretization method. In our previous work [14], we integrated the energy equation (5) and fig. 3 there is affected by such a parasitic flow. Instead, if we use the entropy equation (8), the entropy production rate tends to zero or $\nabla_i v_j \to 0$ and $\nabla_i T \to 0$ at long times if there is no heat flow from outside. Thus, with our new method, equilibrium can be reached around the interface region.

In passing, s_0 in eq. (2) disappears in eq. (8) owing to the continuity equation (4), so it is an arbitrary constant.

Numerical method. – We assume a cylindrical cell with $0 < z < H$ and $0 < r = \sqrt{x^2 + y^2} < L$ filled with a fluid. The system volume $\pi L^2 H$ is thus fixed. In this axisymmetric geometry, we assume that all the variables depend only on z, r, and t. We integrated the dynamic equations on a two-dimensional lattice with $H = 400\Delta x$ and $L = 700\Delta x$, where $\Delta x = \ell/2$ is the mesh size of the integration with

$$\ell = (C/2k_Bv_0)^{1/2}, \quad (10)$$

in terms of C in eq. (1) and v_0 in the van der Waals theory. For $C \sim k_B v_0^{5/3}$, we have $\ell \sim v_0^{1/3}$, but C remains arbitrary in our theory. The interface width in the following simulations is then of order $6\Delta x$, with $\Delta x = \ell/2$ and we obtained almost the same results even for $\Delta x = \ell/4$. We assumed the linear density dependence of the transport coefficients as $\eta = \zeta = \nu_0 mn$ and $\lambda = k_B\nu_0 n$, though they are crude approximations [22]. The kinematic viscosity $\nu_0 = \eta/\rho$ is assumed to be a constant. Space and time will be measured in units of ℓ and

$$\tau_0 = \ell^2/\nu_0 = C/2k_Bv_0\nu_0, \quad (11)$$

respectively. Away from the criticality, the thermal diffusivity $D_T = \lambda/C_p$ is of order ν_0 (where C_p is the isobaric specific heat per unit volume) or the Prandtl number $Pr = \nu_0/D_T$ is of order unity. Hence τ_0 is the thermal relaxation time on the scale of ℓ. There arises a dimensionless number $\sigma \equiv \nu_0^2 m/\epsilon\ell^2$ and we set $\sigma = 0.06$ in this work. Then $\nu_0 = (0.06\epsilon/m)^{1/2}\ell$ or $C = k_Bv_0\nu_0^2 m/0.03\epsilon$. The velocity field $\boldsymbol{v}$ vanishes on all the boundaries. We control the boundary temperatures at $z = 0$ and H, written as T_0 and T_H, while the side wall at $r = L$ is thermally insulating or $(\partial T/\partial r)_{r=L} = 0$. On the substrate $z = 0$ we imposed the boundary condition [8]

$$\frac{\partial n}{\partial z} = -\Phi_1/v_0\ell, \quad (12)$$

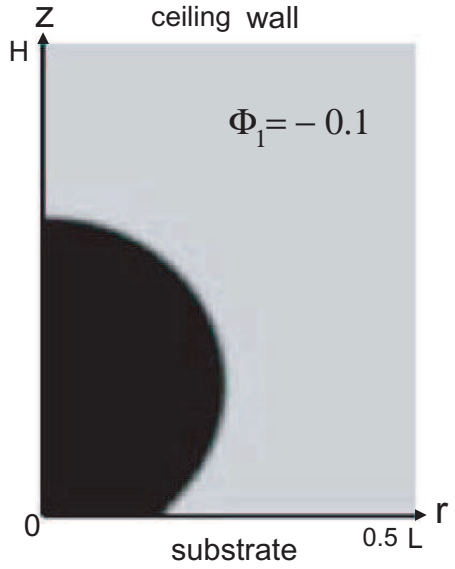

Fig. 1: Axisymmetric liquid droplet (in black) on the substrate in gas (in gray) for $\Phi_1 = -0.1$ and $T = 0.875T_c$ in equilibrium in a cylindrical cell ($0 < z < H$ and $0 < r < L$). Here the region $r < L/2$ is shown. A thermally insulating side wall is at $r = L$. In this work $H = 400\Delta x = 200\ell$ and $L = 700\Delta x = 350\ell$.

where Φ_1 arises from the short-range interaction between the fluid and the wall assumed to be smooth [1]. We set $\partial n/\partial z = 0$ at $z = H$ and $\partial n/\partial r = -0.1/v_0\ell$ at $r = L$.

We first placed a hemispheric liquid droplet with radius 100 at $T = 0.875T_c$, where the liquid and gas densities were those on the coexistence curve given by $n_\ell = 0.580/v_0$ and $n_g = 0.122/v_0$, respectively. We then waited a time interval of 4200 to let the system relax to the true equilibrium, where $T = 0.875T_c$ throughout the system and $\boldsymbol{v} = \boldsymbol{0}$ even around the interface, and the pressure difference between the two phases satisfied the Laplace law. The liquid and gas densities attained are $0.581/v_0$ and $0.123/v_0$, respectively, which are slightly different from the initial values due to the surface tension effect. In fig. 1, we show such a state with $\Phi_1 = -0.1$, where the contact angle is 135°. At $T = 0.875T_c$, the contact angle vanishes for $\Phi_1 \cong 0.12$ and the wall is completely wetted by liquid for larger Φ_1. We determine the interface position by $n(r, z) = (n_\ell + n_g)/2$. As $z \to 0$ we obtain the position of the contact line $r = r_c$.

Heating a liquid droplet. – We prepared an equilibrium state with $\Phi_1 = 0.05$ in the partial wetting condition, where the contact angle is 57°. We then raised the substrate temperature T_0 to $0.91T_c$, while the temperature T_H at the ceiling was unchanged from $0.875T_c$. We set $t = 0$ at this temperature change. The Φ_1 was kept fixed. The contact angle increased up to 67° around $t = 1800$ in accord with the experiment [13], but it slowly decreased afterwards being equal to 60° at $t = 10800$. (These two times correspond to the beginning and middle of a late stage of evaporation in fig. 4 below.) The droplet assumed a cap-like shape until it disappeared.

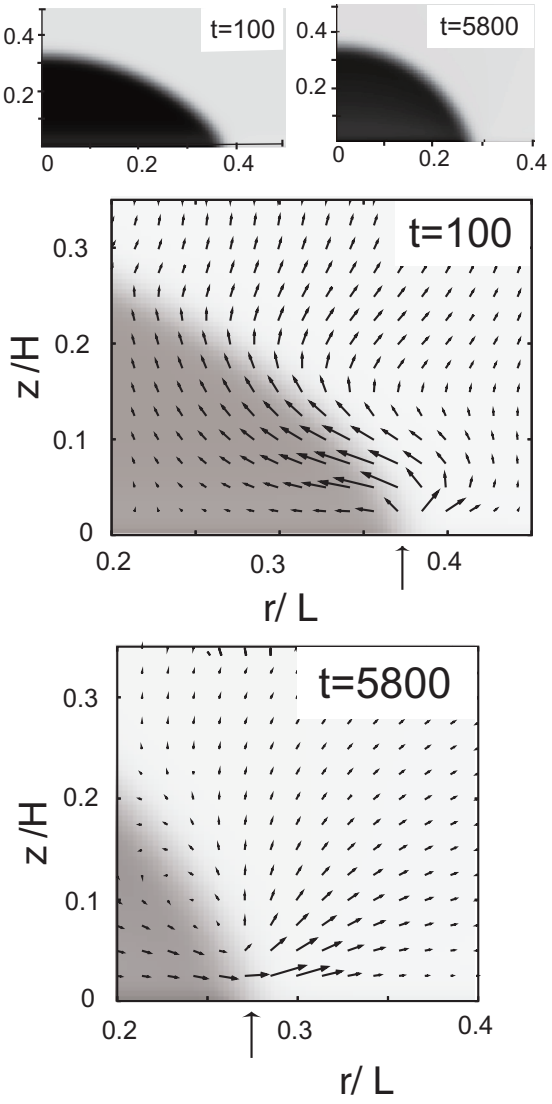

Fig. 2: Droplet shape (top) and velocity field (middle and bottom) for $\Phi_1 = 0.05$ at $t = 100$ and 5800 on a heated substrate with the darker regions representing liquid. Evaporation strongly takes place around the contact line, as can be seen from the velocity field (arrows).

In fig. 2, the droplet shape and the velocity field are shown at $t = 100$ in an early stage and at $t = 5800$ in a late stage. Evaporation is taking place strongly in the vicinity of the contact line $r = r_c(t)$. In the upper panel of fig. 3, we show the heat flux on the substrate

$$Q_{\rm b}(r, t) = -\left(\lambda \frac{\partial T}{\partial z}\right)_{z=0}, \tag{13}$$

at these two times. It exhibits a sharp peak at $r = r_c(t)$, where the wall supplies excess heat needed for evaporation. This behavior is in accord with the theoretical result by Nikolayev *et al.* [11]. In the lower panel of fig. 3 at $t = 5800$, the temperature T is nearly constant along the

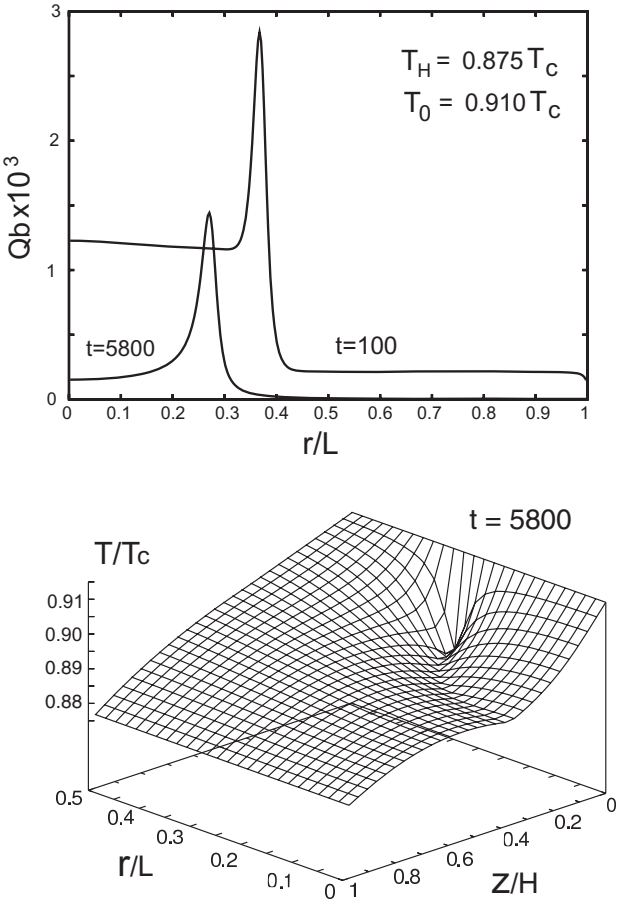

Fig. 3: Upper panel: heat flux $Q_{\rm b}(r,t)$ on a heated substrate in units of $\epsilon\ell/v_0\tau_0$ at $t=100$ and 5800 with a sharp maximum at the contact line $r=r_c(t)$. Lower panel: profile of $T(r,z,t)/T_c$ at $t=5800$. It sharply drops to 0.8815 near the contact line ($r=r_c(t)$ and $z=0$), where evaporation occurs strongly.

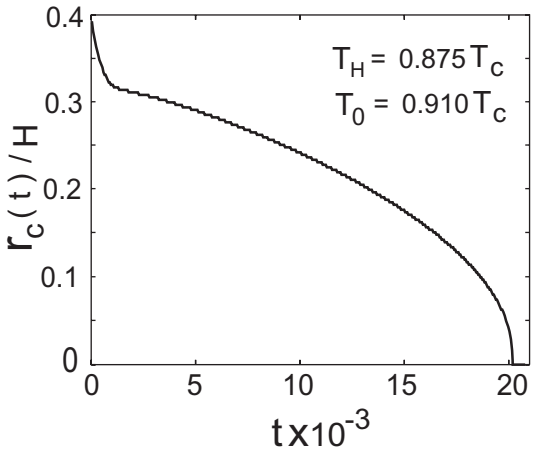

Fig. 4: Time evolution of the contact line radius $r_c(t)$ of an evaporating droplet. For $t\gtrsim 10^3$ it may be fitted to eq. (15). For $t\lesssim 10^3$ it decreases rapidly due to enhanced evaporation.

interface, as in our previous simulation [14]. It is nearly equal to the coexistence temperature $T_{\rm cx}(p)$, where p is the pressure homogeneous outside the interface region, as anlytic calculations demonstrated [15].

In our simulation, T sharply drops from T_0 to $T_{\rm cx}(p)$ near the contact line on the scale of the interface thickness ξ, while T gradually decreases outside the contact line region $|r-r_c|\gg\xi$. We confirmed these results even for other T_0 in the partial wetting condition. The heat flux near the contact line is then given by $Q_{\rm con}=\lambda_\ell\Delta T/\xi$, where $\Delta T=T_0-T_{\rm cx}$ and λ_ℓ is the thermal conductivity of liquid. This heat flux may be equated with the convective latent-heat flux $n_gT_{\rm cx}\Delta s v_g$ in the gas region, where n_g is the gas density, Δs is the entropy difference per particle, and v_g is the gas velocity near the contact line. The convection dominates over the thermal diffusion in this region. Therefore

$$v_g \sim \lambda_\ell\Delta T/(\xi n_gT_{\rm cx}\Delta s) \sim \nu_0 n_\ell\Delta T/\xi n_gT_{\rm cx}. \quad (14)$$

In the second line we set $\lambda_\ell=k_B\nu_0 n_\ell$ and $\Delta s\sim k_B$. This estimation is consistent with the numerical values of v_g in fig. 2. We also changed ΔT and confirmed the linear relationship $v_g\propto\Delta T$ in the partial-wetting condition.

In fig. 4, we display the radius of the contact line $r_c(t)$ *vs.* t. In the early stage $t\lesssim 10^3$, $r_c(t)$ decreases rapidly, where evaporation takes place strongly all over the surface (see fig. 5 below). In the late stage $t\gtrsim 10^3$, it decreases algebraically as

$$r_c(t)\propto(t_0-t)^{0.42}, \quad (15)$$

until it disappears at $t_0\cong 2\times 10^4$. The exponent 0.42 in eq. (15) is smaller than the exponent 0.5 for macroscopic droplets in air [2–4]. The droplet volume decreased as $(t_0-t)^{1.12}$ and the average droplet density $\bar{n}(t)$ slowly decreased roughly as $\bar{n}-n_g\propto(t_0-t)^{0.08}$. The latter is because the droplet interior is gradually heated, as can be seen from the inhomogeneous temperature profile in fig. 3. The interior density approaches the gas density before its disappearance. The droplet interior thus changes in a complicated manner and we cannot present clear explanations of the exponents 0.42, 1.12, and 0.08 at present.

Evaporation rate. – We next examine the evaporation rate. To this end we introduce the mass flux through the interface,

$$J=n(\boldsymbol{v}-\boldsymbol{v}_{\rm int})\cdot\boldsymbol{\nu}, \quad (16)$$

where $\boldsymbol{\nu}=-|\nabla n|^{-1}\nabla n$ is the normal unit vector at the surface from liquid to gas and $\boldsymbol{v}_{\rm int}\cdot\boldsymbol{\nu}(\cong {\rm d}r_c(t)/{\rm d}t)$ is the interface velocity. If J is regarded as a function of the coordinate along the normal direction $\boldsymbol{\nu}$, it is continuous through the interface from the mass conservation, while n and $\boldsymbol{v}\cdot\boldsymbol{\nu}$ change discontinuously. Thus we may determine $J=J(r,t)$ on the interface as a function of r at each time. In the thin interface limit J is related to the discontinuity

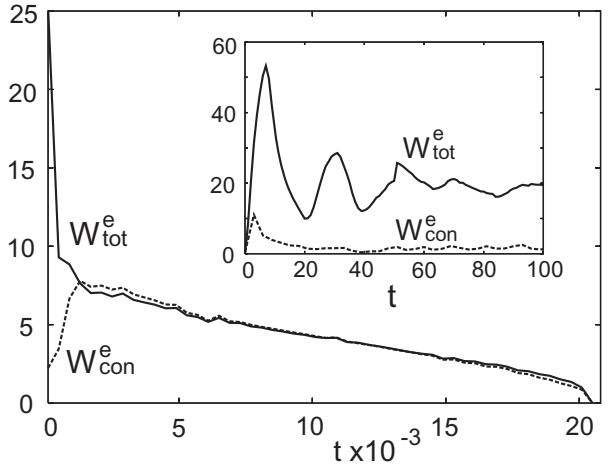

Fig. 5: Evaporation rate $W^e_{\rm tot}$ on all the interface in eq. (18) and that $W^e_{\rm con}$ in the vicinity of the contact line $r_c - 6\ell < r < r_c$ in eq. (19) in units of $\ell^3/v_0\tau_0$ *vs.* t until disappearance of the droplet. Evaporation occurs all over the interface in an early stage after heating the substrate, but it mostly occurs at the contact line in a late stage. Inset: evaporation rates in the early stage, where sound propagation in liquid gives rise to oscillatory relaxation.

of the heat flux $-\lambda\cdot\nabla T$ as

$$T\Delta s J - \boldsymbol{\nu}\cdot[(\lambda\nabla T)_{\rm gas} - (\lambda\nabla T)_{\rm liq}] = 0, \qquad (17)$$

from the energy conservation at the interface, where the subscript gas (liq) denotes the value in the gas (liquid) side close to the interface. The total evaporation rate $W^e_{\rm tot}$ is the surface integral of J. The surface area in the range $[r, r+{\rm d}r]$ is $2\pi {\rm d}r r/\sin\theta$, where θ is the angle between $\boldsymbol{\nu}$ and the r axis. Thus,

$$W^e_{\rm tot} = 2\pi\int_0^{r_c} {\rm d}r r J/\sin\theta. \qquad (18)$$

The particle number within the droplet N_d decreases in time as ${\rm d}N_d/{\rm d}t = -W^e_{\rm tot}$. The droplet volume V_d is related to N_d by $V_d = V_d/\bar{n}$ in terms of the average droplet density $\bar{n}$ and is proportional to r_c^3 for thick droplets. We also define the evaporation rate near the contact line

$$W^e_{\rm con} = 2\pi\int_{r_c-r_w}^{r_c} {\rm d}r r J/\sin\theta. \qquad (19)$$

Here we set $r_w = 6\ell$, which is twice longer than the interface width and remains shorter than r_c before the droplet disappearance. In fig. 5, we show $W^e_{\rm tot}(t)$ and $W^e_{\rm con}(t)$ *vs.* t. The two curves nearly coincide for $t \gtrsim 10^3$. This demonstrates that evaporation occurs only near the contact line at long times. Also in fig. 3, along the interface far from the substrate $z \gg \xi$, we can see $\boldsymbol{\nu}\cdot\nabla T = 0$ and recognize $J = 0$ from eq. (17). In terms of v_g in eq. (14) we then obtain

$$W^e_{\rm tot} \sim 2\pi\xi r_c n_g v_g. \qquad (20)$$

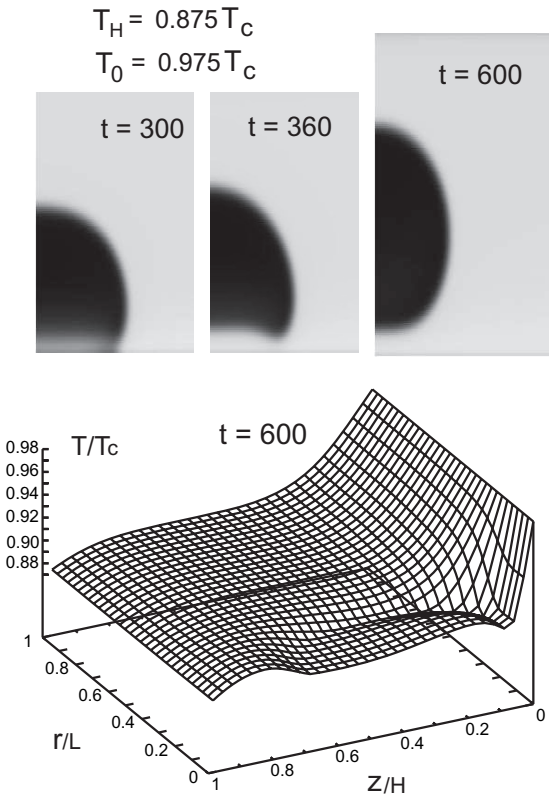

Fig. 6: Leidenfrost effect for $T_0 = 0.975T_c$ and $T_H = 0.875T_c$. Top panels: a gas layer appears between the droplet and the substrate (left) and the droplet is detached from the substrate (middle and right). Bottom panel: profile of $T(r,z,t)/T_c$ at $t = 600$ after droplet detachment, where T is nearly constant along the interface. The gas layer between the droplet and the substrate has a large temperature gradient.

If the droplet density is treated as a constant ($= n_\ell$), eqs. (14) and (21) yield

$$\frac{\rm d}{{\rm d}t} r_c(t)^2 \sim -W^e_{\rm tot}/r_c n_\ell \sim -\lambda_\ell \Delta T/T_{\rm cx} n_\ell \Delta s, \qquad (21)$$

which is consistent with the curve in fig. 4 at long times $t \gtrsim 10^3$. The agreement with the decay behavior (15) becomes better if we account for the slow decrease of the droplet density (see the discussion below eq. (15)).

As shown in the inset of fig. 5, $W^e_{\rm tot}$ is much enhanced exhibiting oscillatory behavior on the acoustic time scale (of the order of the droplet radius divided by the liquid sound velocity), where evaporation takes place all over the interface. The sound velocity is 5.43 in liquid and 2.67 in gas in units of ℓ/τ_0 (with $\sigma = 0.06$) at $T = 0.875T_c$, so the acoutic disturbances propagate faster in liquid. Before the first peak of $W^e_{\rm tot}$, a compression sound pulse emitted from the substrate adiabatically warms the liquid [23,24], resulting in a rapid rise of evaporation on all the interface. Its subsequent sharp drop at $t \sim 7$ then occurs with propagation of an expansion sound wave emitted from the contact line, where evaporation suddenly starts and cools

the surrounding liquid. These acoustic waves are mixed after the first minimum.

Leidenfrost effect. – In fig. 6, we show an extreme case of heating the substrate from $0.875T_c$ to $0.975T_c$ at $t=0$. Here, at the pressure in the gas, the substrate temperature is much above $T_{\rm cx}(p)$ and the thermal diffusion is relatively slow near the substrate since $T_0 \cong T_c$. On a time scale of order 100, a gas layer emerges on the substrate and it supports a large temperature gradient. Here the whole liquid layer adjacent to the heater turns simultaneously into the gas. The droplet is then detached from the substrate (the Leidenfrost effect). Without gravity in this case, the droplet slowly moves towards the cooler boundary and the droplet interior becomes cooler than the surrounding gas region due to evaporation. It eventually collides with the cooler boundary to form a thickened wetting layer (see fig. 7 of our previous paper [14]). In gravity, a droplet may be suspended in gas in a steady state. On the other hand, a gas bubble is attracted to a warmer boundary [13,14]. The lower panel of fig. 6 demonstrates that the temperature is nearly homogeneous all along the interface at $T_{\rm cx}(p)$ with disappearance of the contact line. Here the temperature in the gas layer between the droplet and the substrate steeply changes from T_0 to $T_{\rm cx}(p)$. Thus the layer is strongly absorbing heat from the substrate.

Summary and concluding remarks. – For one-component fluids we have examined evaporation of a small droplet on a heated smooth substrate in the partial wetting condition in the axisymmetric geometry. In the dynamic van der Waals theory [14], we have integrated the entropy equation (8) together with the continuity and momentum equations to avoid parasitic flow around the interface. Our system length is of the order of several ten nanometers if the mesh length Δx is a few Å.

In our simulation, the temperature exhibits a sharp drop near the contact line, leading to a large temperature gradient and a large heat flux localized near the contact line. As is evident in fig. 5, evaporation in one-component fluids occurs only near the contact line at long times. Here we should note that we have assumed the isothermal boundary condition on the substrate. For finite thermal conductivity of the wall, however, the substrate temperature is lowered at the contact line and the temperature drop to $T_{\rm cx}(p)$ in the fluid should become much more gradual near the contact line [11,12,16].

Phenomenologically, the evaporation rate of a thin liquid droplet in air has been assumed to be of the form [2–4],

$$J(r,t) = J_0/\sqrt{r_c(t)^2 - r^2}. \tag{22}$$

Here J_0 is a constant, but its expression in terms of the physical parameters remains unknown. The total evaporation rate $W^e_{\rm tot}$, which is the surface integral of $J(r,t)$, is proportional to r_c as in our case in eq. (20). If the temporal decrease of the liquid density is neglected, the above $J(r,t)$ yields $r_c(t) \propto (t_0 - t)^{0.5}$ in agreement with the experiments [2–4]. This decay law is analogous to that in eq. (21) for one-component fluids, although the forms of $J(r,t)$ in the two cases are very different. In multi-component fluids, a velocity field induced by the Marangoni effect should serve to realize evaporation on all the interface [9,10].

* * *

This work was supported by KAKENHI (Grant-in-Aid for Scientific Research) on Priority Area Soft Matter Physics from the Ministry of Education, Culture, Sports, Science and Technology of Japan.

REFERENCES

[1] de Gennes P. G., *Rev. Mod. Phys.*, **57** (1985) 827.
[2] Deegan R. D., Bakajin O., Dupont T. F., Huber G., Nagel S. R. and Witten T. A., *Nature*, **389** (1997) 827.
[3] Guéna G., Poulard C. and Cazabat A. M., *Colloid Interface Sci.*, **312** (2007) 164.
[4] Shahidzadeh-Bonn N., Rafai S., Azouni A. and Bonn D., *J. Fluid. Mech.*, **549** (2006) 307.
[5] Butt H. J., Glovko D. S. and Bonaccurso E., *J. Phys. Chem B*, **111** (2007) 5277.
[6] Anderson D. M. and Davis S. H., *Phys. Fluids*, **7** (1995) 248.
[7] Koplik J., Pal S. and Banavar J. R., *Phys. Rev. E*, **65** (2002) 021504.
[8] Briant A. J., Wagner A. J. and Yeomans J. M., *Phys. Rev. E*, **69** (2004) 031602.
[9] Savino R. and Fico S., *Phys. Fluids*, **16** (2004) 3738.
[10] Hu H. and Larson R. G., *Langmuir*, **21** (2005) 3972.
[11] Nikolayev V. S., Beysens D. A., Lagier G. L. and Hegseth J., *Int. J. Heat Mass Transfer*, **44** (2001) 3499.
[12] Nikolayev V. S., preprint (arXiv:0709.4631).
[13] Hegseth J., Oprisan A., Garrabos Y., Nikolayev V. S., Lecoutre-Chabot C. and Beysens D., *Phys. Rev. E*, **72** (2005) 031602.
[14] Onuki A., *Phys. Rev. E*, **75** (2007) 036304.
[15] Onuki A. and Kanatani K., *Phys. Rev. E*, **72** (2005) 066304.
[16] Höhmann C. and Stephan P., *Exp. Thermal Fluid Sci.*, **26** (2002) 157.
[17] Landau L. D. and Lifshitz E. M., *Fluid Mechanics* (Pergamon) 1959.
[18] Rowlinson J. S., *J. Stat. Phys.*, **20** (1979) 197.
[19] Lafaurie B., Nardone C., Scardovelli R., Zaleski S. and Zanetti G., *J. Comput. Phys.*, **113** (1994) 134.
[20] Jamet D., Torres D. and Brackbill J. U., *J. Comput. Phys.*, **182** (2002) 262.
[21] Shin S., Abdel-Khalik S. I., Daru V. and Juric D., *J. Comput. Phys.*, **203** (2005) 493.
[22] Bird R. B., Stewart W. E. and Lightfoot E. N., *Transport Phenomena* (Wiley, New York) 2002, p. 272.
[23] Miura Y., Yoshihara S., Ohnishi M., Honda K., Matsumoto M., Kawai J., Ishikawa M., Kobayashi H. and Onuki A., *Phys. Rev. E*, **74** (2006) 010101(R).
[24] Onuki A., *Phys. Rev. E*, **76** (2007) 061126.